Original Article

JCBFM

Journal of Cerebral Blood Flow & Metabolism
2016, Vol. 36(4) 808–818

DOI: 10.1177/0271678X15608390
jcbfm.sagepub.com
SAGE

Graph theoretical analysis of functional networks and its relationship to cognitive decline in patients with carotid stenosis

Ting-Yu Chang[1,*], Kuo-Lun Huang[1,*], Meng-Yang Ho[2], Pei-Shan Ho[3], Chien-Hung Chang[1], Chi-Hung Liu[1], Yeu-Jhy Chang[1], Ho-Fai Wong[4], I-Chang Hsieh[5], Tsong-Hai Lee[1] and Ho-Ling Liu[3,6]

Abstract

Significant carotid stenosis compromises hemodynamics and impairs cognitive functions. The interplay between these changes and brain connectivity has rarely been investigated. We aimed to discover the changes of functional connectivity and its relation to cognitive decline in carotid stenosis patients. Twenty-seven patients with unilateral carotid stenosis (≥60%) and 20 age- and sex-matched controls underwent neuropsychological tests and resting-state functional magnetic resonance imaging. The patients also received perfusion magnetic resonance imaging. The relationships between cognitive function and functional networks among the patients and controls were evaluated. Graph theory was applied on resting-state functional magnetic resonance imaging network analysis, which revealed that the hemispheres ipsilateral to the stenosis were significantly impaired in "degree" and "global efficiency." The neuropsychological performances were positively correlated with degree, clustering coefficient, local efficiency, and global efficiency, and negatively correlated with characteristic path length, modularity, and small-worldness in the patients, whereas these relationships were not observed in the controls. In this study, we identified the networks that were impaired in the affected hemispheres in patients with carotid stenosis. Specific indices (global efficiency, characteristic path length, and modularity) were highly correlated with neuropsychological performance in our patients. Analysis of brain connectivity may help to elucidate the relationship between hemodynamic impairment and cognitive decline.

Keywords

Carotid stenosis, cognitive impairment, functional connectivity, graph theory, hemodynamics, resting state functional magnetic resonance imaging

Received 17 October 2014; Revised 27 May 2015; Accepted 19 June 2015

[1]Department of Neurology, Stroke Section, Chang Gung Memorial Hospital, Linkou Medical Center and College of Medicine, Chang Gung University, Taoyuan, Taiwan
[2]Clinical Psychology Program, c/o Department of Occupational Therapy, Chang Gung University, Taoyuan, Taiwan
[3]Department of Medical Imaging and Radiological Sciences, Chang Gung University, Taoyuan, Taiwan
[4]Department of Medical Imaging and Intervention, Chang Gung Memorial Hospital, Taoyuan, Taiwan
[5]Department of Cardiology, Chang Gung Memorial Hospital, Taoyuan, Taiwan
[6]Department of Imaging Physics, The University of Texas M.D. Anderson Cancer Center, Houston, Texas, USA
[*]Ting-Yu Chang and Kuo-Lun Huang have equal contribution.

Corresponding authors:
Ho-Ling Liu, Department of Imaging Physics, The University of Texas M.D., Anderson Cancer Center, Unit 1472, 1515 Holcombe Boulevard, Houston, TX 77030, USA.
Email: haliu@mdanderson.org and
Tsong-Hai Lee, Department of Neurology, Chang Gung Memorial Hospital, #5 Fuhsing Street, Guishan Township, Taoyuan County, Taiwan.
Email: thlee@cgmh.org.tw

Introduction

Significant carotid stenosis may cause a range of clinical or subclinical complications. Clinically, ischemic stroke or transient ischemic attack may occur in patients with decompensated hemodynamics.[1] Subclinically, poor cerebral vasoreactivity (CVR) may represent a defective reserve capacity for cerebral perfusion.[2] In addition to vascular events, cognitive impairment and white matter lesions (WMLs) are also thought to be overt in patients with carotid stenosis.[3,4] Although cerebral hypoperfusion or silent infarcts may contribute to these deteriorations,[5,6] the mechanisms of subsequently altered brain function (e.g. cognitive decline) or micro-structural changes (e.g. WMLs) have yet to be elucidated.

Functional neuroimaging helps to disclose brain activities and has become important tool in research on neurological diseases. While task-specific functional magnetic resonance imaging (fMRI) detects relative changes from baseline of blood oxygenation level-dependent (BOLD) signals when performing a task or in the response to a stimulus, resting-state fMRI (R-fMRI) is also a promising tool for understanding functional connectivity of the brain.[7] By imaging the brain during rest, R-fMRI detects large-amplitude spontaneous low-frequency fluctuations in BOLD signals that are temporally correlated across functionally related areas. From this basis many cerebral networks that are believed to be functionally correlated during "resting" in the brain have been identified.[8] R-fMRI has also been applied to various clinical conditions,[9] including diagnosis (Alzheimer's disease),[10] delineating pathophysiology (psychiatric diseases),[11] or pre-surgical planning (epilepsy).[12]

The brain functional connectivity of patients with carotid stenosis has rarely been studied.[13] Previous research has demonstrated decreased or asymmetrical functional connectivity of selective networks, including frontoparietal network, default mode network, dorsal attention network, and sensorimotor network in patients with asymptomatic carotid stenosis compared to normal controls.[13,14] However, the impact of unilateral carotid stenosis on the overall functional networks has not been clearly delineated. With the progression of proximal arterial stenosis/occlusion, collateral circulations build up to maintain constant perfusion through complex mechanisms.[15,16] Since cerebral hypoperfusion and impaired hemodynamics may play major roles in cognitive decline in patients with carotid stenosis,[5,17] the disrupted functional networks in this group may be more complicated and widespread. Hence, in the current study, we conducted both perfusion MRI and R-fMRI in patients with significant unilateral carotid stenosis, and carried on graph theoretical analysis of global (whole brain) networks.[18] We investigated the differences in functional connectivity between hemispheres and explored specific brain networks that may be more vulnerable to compromised hemodynamics. The cognitive status according to extensive neuropsychological tests and its relationship to brain connectivity were also examined.

Materials and methods

Subjects

Twenty-seven patients with significant unilateral internal carotid artery (ICA) stenosis ($\geq$60% according to the North American Symptomatic Carotid Endarterectomy Trial NASCET criteria) were prospectively enrolled at Linkou Chang Gung Memorial Hospital, Taiwan. The exclusion criteria included: (1) $\geq$50% intracranial stenosis or contralateral ICA stenosis; (2) stroke within the past 3 weeks; (3) previous stroke producing $\geq$one-third middle cerebral artery (MCA) territory infarction; (4) functional disability (modified Rankin Scale $\geq$ 3); (5) Mini-Mental Status Examination (MMSE) score $<$ 24;[19] (6) co-morbidity with other neurological degenerative or psychiatric disorders; (7) co-morbidity with severe systemic illnesses including heart failure, cirrhosis, renal insufficiency, or malignancy; and (8) allergy to iodinated or gadolinium-based contrast medium. Twenty age- and sex-matched subjects without carotid stenosis as screened by carotid ultrasound were recruited as normal controls.

Ethics statement

Written informed consent was obtained from all subjects. This study was conducted in accordance with the principles expressed in the Declaration of Helsinki, and was approved by the Institutional Review Board of Chang Gung Memorial Hospital.

Neuropsychological assessments

Neuropsychological assessments were performed as described in our previously published article.[20] Briefly, the neuropsychological tests used in the current study included: (1) Raven's Standard Progressive Matrices (SPM): to test current intellectual ability; (2) the Chinese Graded Word Reading Test (CGWRT): to ensure all the subjects had a minimal command of Chinese reading ability; (3) the California Verbal Learning Test-II (CVLT-II) and the Brief Visual Memory Test-Revised (BVMT-R): to assess memory for verbal and visual materials, respectively; (4) the Purdue Pegboard Test (PPT): used to test manual dexterity of both hands; (5) the Benton 3-Dimensional

Construction Praxis Test (B3D): to measure constructional praxis;[21] and (6) the Category Fluency Test (CFT) and Design Fluency Test (DFS): to test the performance of response initiation and the ability to switch responses according to different instructions, respectively.

Image acquisition

All MR images were acquired on a 1.5T clinical scanner (Gyroscan Intera, Philips, Best, the Netherlands) with the SENSE head coil. The scanning protocols included T2-weighted fluid attenuated inversion recovery (FLAIR) scans and R-fMRI for all subjects. In addition, dynamic susceptibility contrast (DSC) perfusion imaging was performed only for patients. The T2-weighted FLAIR images (TR/TE/TI = 9788 ms/90 ms/2300 ms, echo train length = 13, in-plane matrix = 256×256, slice thickness/gap = 5 mm/1.5 mm, total 20 slices) were obtained to examine WMLs and old infarct. Trained neurologists blinded to the clinical and cognitive conditions performed the qualitative and quantitative measurements of the images. The visual grading system reported by Fazekas et al.[22] in 1987 was used to assess the severity of the WMLs. Lacunar infarcts were defined as lesions less than 15 mm in diameter with similar MRI signal characteristics as cerebrospinal fluid (CSF). The severity of cerebral infarct (infarct score) was visually rated as follows: 0, no lesion; 1, one focal lesion ($\geq$5 mm); 2, more than one focal lesion; and 3, confluent lesions.[23]

For the R-fMRI scans, the subjects were asked to keep their eyes closed, not fall asleep, and think about nothing in particular. R-fMRI was implemented using a T_2*-weighted single-shot gradient-echo echo-planar imaging (EPI) sequence (TR/TE/FA = 2000 ms/50 ms/90°, in-plane matrix = 64×64, slice thickness = 5 mm). For each subject, 20 continuous axial slices per volume and a total of 150 volumes were acquired with a total time of 5 minutes.

For DSC-MRI, a single-shot gradient echo EPI sequence was applied with the following parameters: TR/TE/FA = 1500 ms/40 ms/55°, matrix size = 112×84 and FOV = 192 mm × 192 mm. Sixteen milliliters of gadolinium diethylene-triamine penta-acetic acid (Gd-DTPA: Magnevist, Schering, Berlin, Germany) was injected into the patients using a power injector with an injection rate of 4 mL/s.

Data preprocessing

R-fMRI data preprocessing was conducted using SPM8 software (Welcome Department of Cognitive Neurology, Institute of Neurology, London, UK) and REST software (by SONG Xiaowei, YAN Chaogan et al., http://restfmri.net/forum/index.php?q=rest), both implemented in MATLAB (Mathworks, Natick, MA, USA). All functional datasets underwent slice timing correction, realignment for head motion correction, spatial normalization to the Montreal Neurological Institute template, and re-sampled to $2 \times 2 \times 2$ mm^3. Linear trend was then removed and the data were band-pass filtered between 0.04 and 0.08 Hz. To reduce spurious variations of nuisance signals, the time course was regressed from the white matter and CSF signals, and combined with the six–rigid body realignment parameters.

Functional network analysis

To construct the brain functional networks, the pre-processed R-fMRI image of each subject's whole brain was parcellated by the defined automated anatomical labeling (AAL) atlas[24] into 90 regions of interest (ROI) (Supplementary Table 1). The time series of each region were then obtained by averaging the signal intensities of the pre-processed R-fMRI images over all voxels within that ROI. After calculating the Pearson correlation coefficient (r) between each pair of the 90 ROIs, a 90×90 correlation matrix was constructed for each subject. The connections represented undirected edges between regions if r values exceeded a threshold. To inspect how degree was affected by the r-threshold, the correlation matrices were thresholded repeatedly across a range of $r = 0.1$ to 0.8 at intervals of 0.01. For other analysis, the r-thresholds were chosen to match fixed density values (0.1, 0.2, and 0.3). The density was defined as the connected edges divided by the maximum number of possibly connected edges of the whole brain, and the range of 0.1 to 0.3 was found to be reliable.[25] In addition to the whole brain network analysis, we divided the brain into two hemispheres and treated them independently. Therefore a 45×45 correlation matrix was obtained for each hemisphere for each subject.

Graph theory was applied to estimate network parameters using BCT software (https://sites.google.com/site/bctnet/).[26] Four node-based and five global parameters were obtained for each network. The node-based network parameters included degree, clustering coefficient (C), local efficiency (E_{loc}), and betweenness centrality (BC), and the global parameters included characteristic path length (L), global efficiency (E_{glob}), modularity (Q), small-worldness (σ), and assortativity coefficient (A). Mathematical definitions of these parameters can be found in the study by Rubinov and Sporns,[26] and the brief descriptions were addressed in Data Supplement. For the node-based parameters, mean values were calculated by averaging across each hemisphere (45×45 correlation matrix) and across the

whole brain (90×90 correlation matrix) for each subject.

Perfusion analysis

Perfusion images were analyzed using Perfusion Mismatch Analyzer software (Ver. 3.0.0.0; Acute Stroke Imaging Standardization Group-Japan; http://asist.umin.jp/index-e.htm). Arterial input functions were carefully chosen from the contralateral MCA to quantify relative cerebral blood flow (CBF) maps using the block-circulant singular value decomposition deconvolution algorithm.[27] A previously described ROI template[2] was spatially transferred to the image space of each patient by using SPM8 software to determine averaged relative CBF values in the relevant regions. The spatial transformation was performed by using the normalization procedure with nearest neighborhood interpolation for re-sampling the ROI mask. The relative CBF values obtained from either side of MCA territories were then divided by the mean value of the bilateral occipital white matter ROI,[2] with the ratios represented as normalized CBF (nCBF) values. Other parameters including time-to-maximum of the residue function (Tmax), mean transit time (MTT), and time to peak (TTP) were also obtained.

Statistical analysis

Data were analyzed using the Statistical Package for Social Sciences (IBM SPSS version 20.0 for Windows). Paired t-tests were performed to assess the node-based parameters between two hemispheres. Two-sample t-tests were used to measure the differences in whole brain-averaged node-based and global network parameters between the patients and controls. Pearson correlation coefficients were calculated to assess correlations between network parameters and neuropsychological tests. Because cognitive functions are strongly associated with age[28] and recent evidences also showed that global functional connectivity may be related to age,[29] correlations between connectivity and cognition could be jointly moderated by age. Hence, partial correlation coefficients were calculated subsequently after controlling for age. For all statistical analysis, a p value of less than 0.05 was considered to be statistically significant.

Results

The average stenotic severity of the patients was 79.2%. There were 12 and 15 patients with left and right ICA stenosis, respectively. Demographic data of the patients and controls shows no significant differences in years of education, diabetes mellitus, hyperlipidemia, and infarct scores between the two groups. However, hypertension (76% vs 35%, $p = 0.005$) and the grading of WMLs (0.96 ± 0.58 vs. 0.55 ± 0.51, $p = 0.02$) were significantly higher in the patients (Supplementary Table 2).

The detailed results of the neuropsychological tests and comparisons between the patients and controls are demonstrated in Table 1. Although the MMSE scores were quite similar between the two groups, the patients had significantly worse performance in many aspects of the neuropsychological tests, especially in current intellectual ability (SPM, $p < 0.01$), visual memory (BVMT-R, $p < 0.01$), manual dexterity (PPT, $p < 0.01$), and the ability of problem solving responses (DFS, $p < 0.01$).

Figure 1(a and b) illustrates the typical brain networks derived from R-fMRI of two patients. Sparser functional connectivity was observed in the hemisphere of the stenotic side in these patients. To demonstrate group differences, correlation matrices were averaged and thresholded for the patients and controls. The correlation matrices of the patients with right-side stenosis were left-right flipped before averaging with those of the patients with left-side stenosis. The averaged connectivity map of the patients exhibited pronounced asymmetry compared to that of the controls (Figure 1c and d). In addition, the density was lower in the patients (0.20) than in the controls (0.31) with the same threshold of the correlation coefficient ($r = 0.36$).

Four node-based network parameters: degree, C, E_{loc}, and BC, were averaged across hemispheres and compared between the ipsilateral and contralateral side of stenosis in the patients, and also between the left and right side in the controls (Table 2). In the controls, there were no differences in any of the four connectivity parameters between the two hemispheres, whereas the patients had significantly less degree and E_{loc} in the ipsilateral hemisphere. Figure 2 illustrates the reduction in degree for the hemisphere ipsilateral to the stenotic side in the patients, both across a wide range of the r threshold (a) and at three fixed density levels (b).

Although many differences in neuropsychological performance between the patients and controls were observed, there were non-significant differences in each global network parameter between the two groups (data not shown). In the analysis when two hemispheres were considered separately (by using 45×45 correlation matrix) with density controlled (0.1, 0.2, and 0.3), E_{glob} was significantly different between the two (affected and non-affected) hemispheres in the patients (only with density = 0.2), but not in the controls (Figure 3). The affected (ipsilateral) hemisphere of the patients exhibited higher hemispheric E_{glob} at lower threshold for controlling the density (mean r-threshold = 0.49 in affected v.s.0.54 in unaffected side).

Table 1. Neuropsychological test.

	Patients (n = 27)	Controls (n = 20)	*p* Value
MMSE	26.11 ± 3.08	27.60 ± 1.82	0.061
SPM_T	24.04 ± 8.84	32.45 ± 8.23	0.002[a]
CGWRT	124.08 ± 30.67	140.15 ± 18.93	0.047[b]
California Verbal Learning Test-II			
Imm. Recall	32.56 ± 9.90	39.15 ± 8.44	0.022[b]
LDF Recall	5.76 ± 4.18	8.60 ± 2.39	0.010[b]
Recogn. Discr	1.8 ± 1.00	2.16 ± 1.01	0.245
Brief Visual Memory Test-Revised			
Imm. Recall	12.56 ± 6.77	18.15 ± 7.43	0.010[b]
Delay Recall	4.93 ± 3.25	8.05 ± 3.62	0.003[a]
Recogn. Discr	4.16 ± 1.62	5.60 ± 0.75	0.001[a]
B3D_Total	19.80 ± 7.55	21.90 ± 4.23	0.273
Purdue Pegboard Test			
Dominant	11.81 ± 2.14	14.50 ± 2.30	0.0002[a]
Non-dominant	10.60 ± 3.49	13.57 ± 2.24	0.002[a]
Category Fluency	35.84 ± 11.36	38.35 ± 6.57	0.386
Design Fluency Test			
Filled Dot	4.68 ± 2.25	7.35 ± 2.96	0.001[a]
Empty Dot	5.84 ± 2.66	8.45 ± 2.58	0.002[a]
Switch	4.88 ± 2.74	7.00 ± 2.88	0.016[b]

MMSE: Mini Mental Status Examination; SPM_T: Raven's Standard Progressive Matrices; CGWRT: Chinese Graded Word Reading Test; Imm. Recall: Immediate Recall; LDF: Long Delay Free Recall; Recogn. Discr: Recognition Discriminability; B3D: Benton 3-Dimensional Construction Praxis Test. [a] < 0.01. [b] $p < 0.05$.

To investigate the relationship between the quantified neuropsychological performance and functional connectivity, partial correlation (age-controlled) of the neuropsychological tests and the nine network parameters was subsequently performed in the two groups. In this part, all network parameters were analyzed at r-threshold = 0.54 under fixed average density = 0.2. In the controls (Supplementary Table 3), only "immediate recall" of the BVMT-R was significantly correlated with several network parameters: positively correlated with degree, C and E_{glob} ($r = 0.46$–0.52), and negatively correlated with BC, L, and σ ($r = -0.492$–0.556). The other neuropsychological results were not correlated with functional connectivity. In contrast, in the patients with carotid stenosis (Table 3), a high correlation of cognitive performance with functional connectivity was found in many of the tests. MMSE, reading ability (CGWRT), and verbal and visual memory ability (CVLT-II and BVMT-R) were all positively correlated with degree, C, E_{loc}, and E_{glob}, and negatively correlated with L, Q, and σ. Among all the nine network parameters, L, E_{glob}, and Q showed the highest correlation with various neuropsychological tests.

Considering co-linear relationship may exist among the network parameters or the neuropsychological tests, the variance inflation factor (VIF) method was subsequently used to test collinearity. After VIF test, C, Q, σ, and A showed low collinearity among the network parameters, and there was low collinearity among 16 neuropsychological tests. Then, C, Q, σ, and A along with age, L, and E_{glob} were taken as variables for stepwise multiple linear regression to test the relationship with neuropsychological data (Table 3 and Supplementary Table 3). In the patients, L, Q, and E_{glob} remained significant predictors (negative correlation for L and Q; positive correlation for E_{glob}) for CVLT and BVMT ($p < 0.05$); in the controls, all network parameters showed no significance except for σ which was negatively correlated with BVMT. Figure 4 demonstrates that BVMT was positively correlated with E_{glob} and negatively correlated with Q in the patients.

Perfusion indices derived from DSC-MRI for each hemisphere of the patients are listed in Supplementary Table 4. Although in the ipsilateral hemisphere, Tmax, MTT, and TPP were significantly longer than in the contralateral hemisphere, nCBF was similar between two hemispheres.

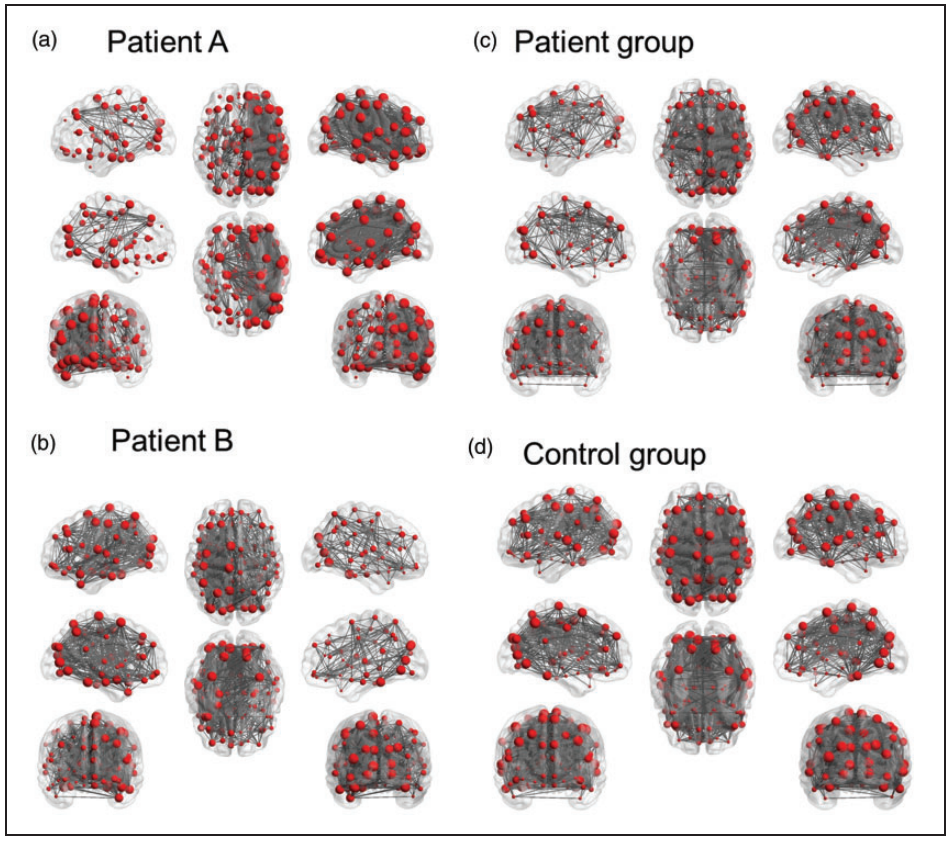

Figure 1. (a and b) The connectivity maps of two patients. Patient A had left internal carotid artery (ICA) 90% stenosis (b), and patient B had right ICA 71% stenosis (b). (Patient A: *r* threshold = 0.60, density = 0.20; Patient B: *r* threshold = 0.41, density = 0.20); (c and d): the averaged connectivity maps of patients (c) and controls (d). The connectivity matrices of the patients with right-side stenosis were left-right flipped before averaging with those with left-side stenosis. (Patients: *r*-threshold = 0.36, density = 0.20; Healthy controls: *r*-threshold = 0.36, density = 0.31).

Table 2. Node-based network parameters averaged across hemispheres (*r* threshold = 0.54).

	Patients (n = 27)			Controls (n = 20)		
	Ipsi^{+}	Contra^{+}	P	Ipsi^{+}	Contra^{+}	P
Degree	15.67 ± 14.1	18.46 ± 15.5	0.008[a]	18.94 ± 11.8	19.73 ± 12.7	0.12
C	0.48 ± 0.2	0.51 ± 0.2	0.07	0.54 ± 0.1	0.54 ± 0.1	0.58
E_{loc}	0.57 ± 0.2	0.62 ± 0.2	0.03[a]	0.68 ± 0.1	0.67 ± 0.1	0.44
BC	102.84 ± 42.8	117.59 ± 49.6	0.09	97.06 ± 32.6	104.27 ± 35.9	0.30

$^{+}$Ipsi.: ipsilateral to stenotic side; Contra.: contralateral to stenotic side; C = clustering coefficient; E_{loc} = local efficiency; BC = Betweenness centrality.
[a]$p < 0.05$.

Discussion

To the best of our knowledge, this prospective R-fMRI study is the first to comprehensively analyze whole brain functional connectivity by graph theory network analysis in patients with unilateral carotid stenosis. For node-based network parameters, the analysis was conducted within a single hemisphere and compared between right and left (in the controls) or ipsilateral and contralateral (in the patients). As shown in Table 2, we found that in the controls, four connectivity parameters (degree, C, E_{loc}, and BC) were similar, while in the patients with significant unilateral carotid stenosis, the functional connectivity of the ipsilateral hemisphere (stenotic side) was decreased, especially in degree ($p = 0.01$) and E_{loc} ($p = 0.03$). Degree is an

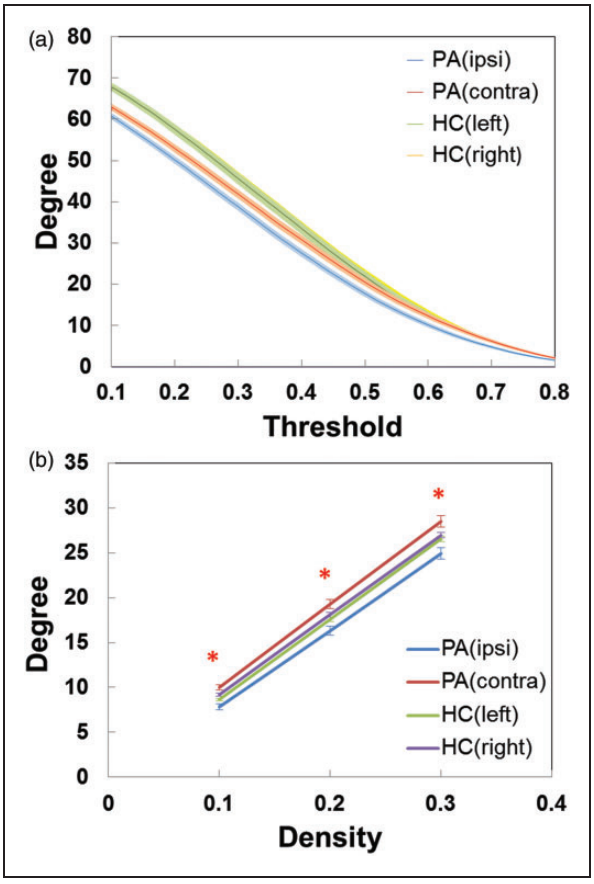

Figure 2. (a) The relationship between the *r* threshold and the mean degree of functional connectivity in either hemisphere of the patients and normal controls. The solid line represents the averaged values across subjects, and the light-colored area indicates the range of one standard deviation. (b) The mean degree of functional connectivity in either hemisphere of the patients and normal controls at three density levels (0.1, 0.2, and 0.3) by node-based analysis. The solid line represents the averaged values across subjects, and the error bar indicates the range of one standard deviation. The red asterisks represent significant differences ($p < 0.05$) from paired t-tests in patients between ipsi- and contra-lateral hemispheres. (Ipsi: ipsilateral to stenosis; Contra: contralateral to stenosis; PA: patients; HC: healthy controls).

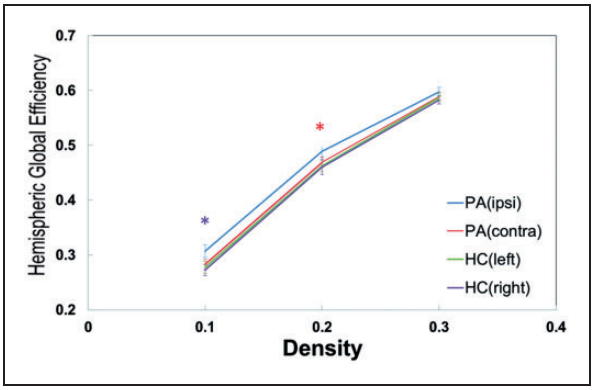

Figure 3. Global efficiency of either hemisphere of the patients and normal controls at three density levels (0.1, 0.2, and 0.3) based on the analysis with two hemispheres considered as separate networks. The solid line represents the averaged values across subjects and the error bar indicates the range of one standard deviation. The red and purple asterisks represent significant ($p < 0.05$) and marginally significant ($p = 0.08$) differences, respectively, from paired t-tests in patients between ipsi- and contra-lateral hemispheres. When density was controlled at 0.2, the *r*-threshold of patients' ipsilateral hemisphere was 0.49; of patients' contralateral and controls' either hemisphere was 0.54. (Ipsi: ipsilateral to stenosis; Contra: contralateral to stenosis; PA: patients; HC: healthy controls).

important marker of network development and resilience,[26] and local efficiency measures the ability of a network to transmit information locally.[30] Our results may indicate that the integrity and efficiency of functional networks are decomposed at the hemodynamically impaired region (the hemisphere ipsilateral to the stenosis), as asymmetry of connectivity was clearly observed in the patients.

In the analysis of the global network parameters, no significance was shown between the controls and patients. Only when we processed each hemisphere independently (by using 45×45 correlation matrix), a significant difference was found in the patients in global efficiency (Figure 3). Global network analysis may not reflect the subtle changes of connectivity in unilateral carotid stenosis, although E_{glob} of the affected hemisphere may be a relatively sensitive index for this specific patient population. There were two considerations needed to be noted from the results of Figure 3: 1. Studies have pointed that measurements in graph theoretical analysis would differ if network size (i.e. density or degree) is changed.[31] The significant discrepancy of hemispheric E_{glob} between two hemispheres in our patients was only found under density = 0.2. A larger cohort of patients will be needed to verify the consistency of the alteration of hemispheric global efficiency; 2. In Figure 3 the value of E_{glob} in patients was higher than in controls. Because this analysis was under controlled density, the *r* threshold of patients' affected side was lower than the unaffected side. Hence, this result only indicated the asymmetry of E_{glob} in unilateral carotid stenosis but did not imply that patients could have higher global efficiency than controls. Whether this finding was related to mechanisms such as a compensatory effect requires further investigation. We speculate that functional connectivity was indeed disrupted in the patients with significant carotid stenosis, not in a global pattern, but limited to the area influenced by compromised hemodynamics. Deterioration of hemodynamics not only increases the risk of ischemic events but also changes the connections of brain activity.

Table 3. Partial correlation coefficient of neuropsychological data and network parameters in patients (n = 27).

	Degree	C	E^{loc}	BC	L	E^{glob}	Q	σ	A
MMSE	.46[a]	.46[a]	.49[a]	–.12	–.51[a]	.57[b]	–.59[b,c]	–.53[a]	–.17
SPM_T	.14	.22	.27	–.22	–.32	.25	–.29	–.23	–.33
CGWRT	.57[b]	.62[b]	.61[b]	–.27	–.56[b]	.63[b]	–.59[b]	–.44[a]	–.24
California Verbal Learning Test-II									
Imm. Recall	.36	.46[a]	.52[a]	–.15	–.54[a,c]	.53[a]	–.55[a]	–.52[a]	–.20
LDF Recall	.27	.36	.44[a]	–.25	–.51[a,c]	.45[a]	–.49[a]	–.52[a]	–.23
Recogn. Discr	.23	.25	.33	–.15	–.42	.41	–.47[a,c]	–.40	–.24
Brief Visual Memory Test-Revised									
Imm. Recall	.38	.31	.34	–.16	–.47[a]	.50[a]	–.62[b,c]	–.50[a]	–.31
Delay Recall	.29	.22	.23	–.41	–.37	.34	–.46[a]	–.19	–.35
Recogn. Discr	.51[a]	.50[a]	.53[a]	–.24	–.58[b]	.63[b,c]	–.58[b]	–.49[a]	–.41
B3D_Total	.42	.36	.37	–.33	–.49[a]	.50[a]	–.51[a,c]	–.37	–.43
Purdue Pegboard Test									
Dominant	–.01	.06	.12	–.02	–.15	.16	–.24	–.29	.05
Non–dominant	.29	.30	.32	–.20	–.39	.48	–.48[a]	–.33	–.15
Category Fluency	.34	.40	.44[a]	–.24	–.46[a]	.46[a]	–.36	–.42	–.27
Design Fluency Test									
Filled Dot	.16	.21	.27	.01	–.30	.30	–.33	–.39	–.03
Empty Dot	.33	.39	.41	–.27	–.48[a]	.44[a]	–.49[a]	–.39	–.21
Switch	.32	.46[a]	.53[a]	–.29	–.58[a,b]	.53[a]	–.42	–.38	–.31

[a]$p < 0.05$ after multiple linear regression analysis. [b]$p < 0.01$ after multiple linear regression analysis. [c]$p < 0.05$ after multiple linear regression analysis. MMSE: Mini Mental Status Examination; SPM_T: Raven's Standard Progressive Matrices; CGWRT: Chinese Graded Word Reading Test; Imm. Recall: Immediate Recall; LDF: Long Delay Free Recall; Recogn. Discr: Recognition Discriminability; Imm. Recall: Immediate; Recogn. Discr: Recognition Discriminability; B3D: Benton 3-Dimensional Construction Praxis Test; PPT: Purdue Pegboard Test; C: clustering coefficient; E_{loc}: local efficiency; BC: Betweenness centrality; L: characteristic path length; E_{glob}: global efficiency; Q: modularity; σ: small-worldness; A: assortativity. (All network parameters were analyzed at *r*-threshold: 0.54.)

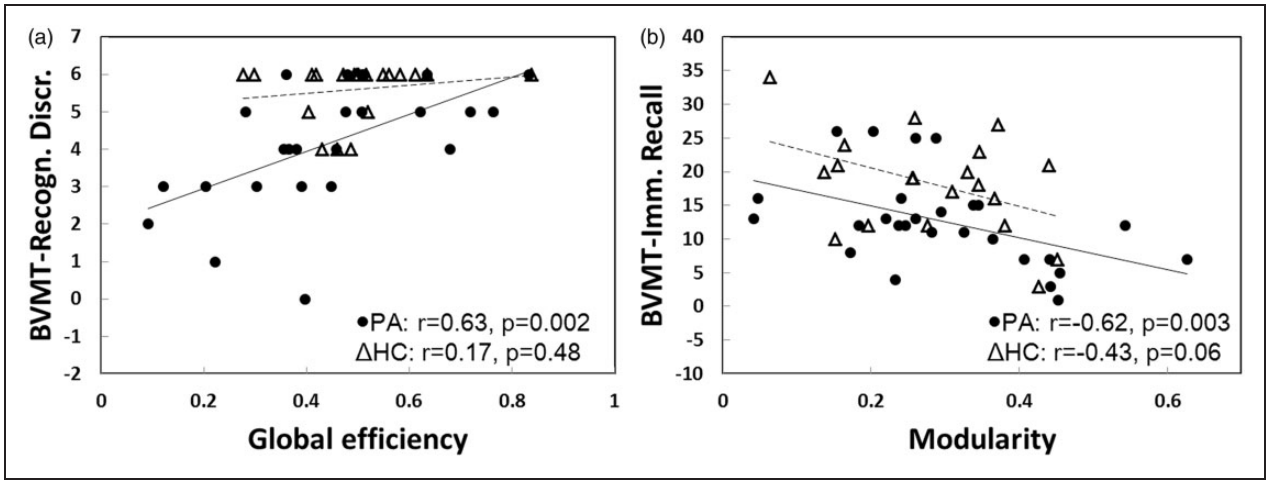

Figure 4. Correlations between BVMT with global efficiency (a) and modularity (b) in the patients and controls. Solid and dashed lines represent linear regressions for the patients and the controls, respectively. (BVMT-Recogn.Discr: BVMT-Recognition Discriminability; BVMT-Imm. Recall: BVMT-Immediate Recall) (patients and controls: density = 0.2, *r*-threshold = 0.54).

The assumption that fluctuations in BOLD signals represent the neural activity is based on the phenomenon of neurovascular coupling. One concern of this study was that our patients were already hemodynamically impaired, and the R-fMRI results might be more interfered by the compromised hemodynamics than the neural activity. Most recently, a study demonstrated that the R-fMRI connectivity of the default mode network could be increased in patients with Moyamoya disease after considering the time delay during the correlation analysis.[32] To test whether such property also existed in our patients, we implemented the delay-correction strategy for analyzing our dataset. The results did not show significant improvement in the connectivity of the affected side and the R-fMRI findings of this study remained unchanged after the correction (data not shown). While it is still debatable whether a simple delay is able to correct for the potential hemodynamic effects on the R-fMRI analysis, to the best of our knowledge, no study reported the evidence of neurovascular uncoupling is a temporal dynamic fashion in the patients with ICA stenosis and intact CBF. The correlation between the impaired functional connectivity indices and the cognitive declines in this study supported that the R-fMRI findings might truly reflect the alteration in neural activity. A study on characterizing the temporal dissociations of the BOLD responses in this patient group is underway.

Our patients had a similar level of education and average age as the controls. However, they had more WMLs and worse performance on various neuropsychological tests. It is believed that significant carotid stenosis is associated with cognitive decline[3] and increased WMLs.[4] Studies also reported that in patients with carotid stenosis, the risk of cognitive regress increases significantly when hemodynamics are impaired.[5] However, how compromised hemodynamics trigger cognitive decline remains unclear. In this study, node-based network parameters including degree and E_{loc} were significantly decreased only in the stenotic hemisphere. Since changes of functional connectivity are generally considered to be related to dementia or cognitive decline,[33,34] the local disruption of brain connectivity in our patients may be a clue to explain the mechanisms of impaired cognitive function with compromised hemodynamics.

Although our patients showed lower psychological functions than controls, there were no differences found between the patients and controls in global network parameters. Global network parameters may not be sensitive enough to detect or to explain the changes in cognitive performance of the patients. However, many neuropsychological tests were highly correlated with some parameters in the patients but not in the controls, even after multiple linear regression analysis. Overall, neuropsychological performance was positively correlated with global efficiency and negatively correlated with characteristic path length and modularity in the patients. Global efficiency is the ability of a network to communicate globally.[35] Our patients had more profound decreases in global efficiency when scores on the neuropsychological tests worsened, especially in visual memory (BVMT-R). Global efficiency may therefore be a sensitive parameter for the regression of specific cognitive functions. Characteristic path length is the average of all shortest paths between each possible pair in a network[36] and may represent how close the inward connections are. It is reasonable that a worse neuropsychological performance may be related to a longer characteristic path length (negatively correlated). Modularity is the degree to which a network is organized into a "modular" structure, i.e. a set of nodules with denser links with each other than with the rest of the network.[37] It was also inversely correlated with neuropsychological functions in our patients. We assume that a higher value of modularity may reflect more "inside" links and less "outside" connections around the nodes, and this seemed to be related to impaired cognitive behavior. Meanwhile, in control, but not in patients, only small-worldness showed negative relation to BVMT-R. Small-worldness network represents high cluster and short path length topology,[36] and the changes of small-worldness connectivity in cognitive decline were not consistent in literature.[38] The existence of negative correlation between small-worldness and visual memory (BVMT) in healthy subjects needs to be further studied. A larger sample size would be needed to clarify whether these parameters differ between the patients and controls. In summary, we suggest that global efficiency, characteristic path length, and modularity may be highly associated with neuropsychological performance and serve as potential predictors of cognitive function deterioration in patients with carotid stenosis.

It is worth noting that in the current study, although the average MMSE scores of the patients and controls were similar, the patients had significantly lower scores on almost all of the other neuropsychological tests. This may imply that the decline in cognitive function in patients with carotid stenosis could be subtle and so cannot be detected by brief mental tests. In such cases, patients would be identified as being "asymptomatic". Hence, when evaluating non-stroke patients with significant carotid stenosis, the definition of "asymptomatic" may be vague and difficult to clarify without detailed neuropsychological assessment.

In perfusion analysis of the patients, the nCBF of either hemisphere was similar, meaning that the blood flow of the stenotic hemisphere remained stationary.

However, there were obvious increases of other parameters including Tmax, MTT, and TTP, indicating compromised hemodynamics of the stenotic hemisphere in the patients.

There are several limitations to this study. First, the sample size was small. Brain networks are complicated and divergent. To investigate possible differences in global connectivity between controls and patients, more subjects would be needed for a comprehensive analysis. Small sample size also limited the analysis of the specific neuropsychological tests in right or left stenosis, respectively. Specific neuropsychological tests (e.g. verbal ability, memory, spatial function...) may evaluate specific hemispheric dysfunction. However, the sample size was too small (15 right and 12 left stenosis) to see the difference or trend in either group. Second, we did not perform correction for physiological factors like heart rate or respiration to the BOLD signal timecourse in preprocessing the R-fMRI data. Although the blood pressure of our subjects was strictly controlled, the BOLD signals might still be interfered by other physiological conditions due to its hemodynamic nature.[39] Third, we only evaluated cerebral perfusion but not CVR in this study. CVR is a practical indicator for hemodynamic status and may be heterogeneous in patients with carotid stenosis.[40] Taking consideration to both CVR changes and R-fMRI, these two parameters may provide more information on the implication of R-fMRI findings in such hemodynamically compromised patients. We are currently conducting studies to clarify the influence of hemodynamics, perfusion status and CVR on brain connectivity. Aside from R-fMRI, electroencephalography or other electrophysiological tools may be needed to provide neuronal information. Fourth, although high correlations between neuropsychological performance and global connectivity in the patients with carotid stenosis were observed, the detailed relationship of selected brain connectivity indices and cognitive functions should be studied further.

Conclusion

Patients with significant unilateral carotid stenosis may have impaired functional connectivity of the affected hemisphere, especially in degree and local efficiency. Compromised hemodynamics may contribute to disruption of hemispheric connectivity. Among complex global networks, global efficiency, characteristic path length, and modularity were highly correlated with the performance on neuropsychological tests in the patients. Further investigations are needed to delineate the relationships between hemodynamic changes, cognitive deteriorations, and functional connectivity alterations.

Funding

The authors disclosed receipt of the following financial support for the research, authorship, and/or publication of this article: The National Science Council (Taiwan) financially supported TYC and KLH with grant number 102-2314-B-182A-055 and 102-2314-B-182A-114. TYC, KLH, and THL were supported by the Chang Gung Medical Research Fund: CMRPG3D0201, CMRPG3B0613, and CMRPG3A0352.

Acknowledgements

We thank Ms Shu-Yu Chou, Ms Yun-Ting Chiang, and the Magnetic Resonance Imaging Center of Chang Gung Memorial Hospital for their kind support in imaging arrangement and technical assistance. We also give special thanks to Dr Changwei W Wu who generously shared experiences with us.

Declaration of conflicting interests

The authors declared no potential conflicts of interest with respect to the research, authorship, and/or publication of this article.

Supplementary material

Supplementary material for this paper can be found at http://jcbfm.sagepub.com/content/by/supplemental-data

References

1. Yonas H, Smith HA, Durham SR, et al. Increased stroke risk predicted by compromised cerebral blood flow reactivity. *J Neurosurg* 1993; 79: 483–489.
2. Chang TY, Liu HL, Lee TH, et al. Change in cerebral perfusion after carotid angioplasty with stenting is related to cerebral vasoreactivity: a study using dynamic susceptibility-weighted contrast-enhanced mr imaging and functional mr imaging with a breath-holding paradigm. *Am J Neuroradiol* 2009; 30: 1330–1336.
3. Mathiesen EB, Waterloo K, Joakimsen O, et al. Reduced neuropsychological test performance in asymptomatic carotid stenosis: the tromso study. *Neurology* 2004; 62: 695–701.
4. Romero JR, Beiser A, Seshadri S, et al. Carotid artery atherosclerosis, mri indices of brain ischemia, aging, and cognitive impairment: The framingham study. *Stroke* 2009; 40: 1590–1596.
5. Balestrini S, Perozzi C, Altamura C, et al. Severe carotid stenosis and impaired cerebral hemodynamics can influence cognitive deterioration. *Neurology* 2013; 80: 2145–2150.
6. Markus HS, King A, Shipley M, et al. Asymptomatic embolisation for prediction of stroke in the asymptomatic carotid emboli study (aces): A prospective observational study. *Lancet Neurol* 2010; 9: 663–671.
7. Ogawa S, Tank DW, Menon R, et al. Intrinsic signal changes accompanying sensory stimulation: Functional brain mapping with magnetic resonance imaging. *Proc Nati Acad Sci U.S.A.* 1992; 89: 5951–5955.

8. Biswal BB, Mennes M, Zuo XN, et al. Toward discovery science of human brain function. *Proc Nati Acad Sci U.S.A*. 2010; 107: 4734–4739.
9. Castellanos FX, Di Martino A, Craddock RC, et al. Clinical applications of the functional connectome. *NeuroImage* 2013; 80: 527–540.
10. Koch W, Teipel S, Mueller S, et al. Diagnostic power of default mode network resting state fmri in the detection of alzheimer's disease. *Neurobiol Aging* 2012; 33: 466–478.
11. Bassett DS, Nelson BG, Mueller BA, et al. Altered resting state complexity in schizophrenia. *NeuroImage* 2012; 59: 2196–2207.
12. Liu H, Buckner RL, Talukdar T, et al. Task-free presurgical mapping using functional magnetic resonance imaging intrinsic activity. *J Neurosurg* 2009; 111: 746–754.
13. Cheng HL, Lin CJ, Soong BW, et al. Impairments in cognitive function and brain connectivity in severe asymptomatic carotid stenosis. *Stroke* 2012; 43: 2567–2573.
14. Lin CJ, Tu PC, Chern CM, et al. Connectivity features for identifying cognitive impairment in presymptomatic carotid stenosis. *PLOS One* 2014; 9: e85441.
15. Romero JR, Pikula A, Nguyen TN, et al. Cerebral collateral circulation in carotid artery disease. *Curr Cardiol Rev* 2009; 5: 279–288.
16. Liebeskind DS. Collateral circulation. *Stroke* 2003; 34: 2279–2284.
17. Silvestrini M, Paolino I, Vernieri F, et al. Cerebral hemodynamics and cognitive performance in patients with asymptomatic carotid stenosis. *Neurology* 2009; 72: 1062–1068.
18. Bullmore E and Sporns O. Complex brain networks: graph theoretical analysis of structural and functional systems. *Nat Rev Neurosci* 2009; 10: 186–198.
19. Lopez MN, Charter RA, Mostafavi B, et al. Psychometric properties of the folstein mini-mental state examination. *Assessment* 2005; 12: 137–144.
20. Huang KL, Chang TY, Chang CH, et al. Relationships between ophthalmic artery flow direction and cognitive performance in patients with unilateral carotid artery stenosis. *J Neurol Sci* 2014; 336: 184–190.
21. Benton AL and Fogel ML. Three-dimensional constructional praxis. A clinical test. *Arch Neurol* 1962; 7: 347–354.
22. Fazekas F, Chawluk JB, Alavi A, et al. MR signal abnormalities at 1.5 t in alzheimer's dementia and normal aging. *AJR Am J Roentgenol* 1987; 149: 351–356.
23. Wahlund LO, Barkhof F, Fazekas F, et al. A new rating scale for age-related white matter changes applicable to MRI and CT. *Stroke* 2001; 32: 1318–1322.
24. Tzourio-Mazoyer N, Landeau B, Papathanassiou D, et al. Automated anatomical labeling of activations in spm using a macroscopic anatomical parcellation of the mni mri single-subject brain. *NeuroImage* 2002; 15: 273–289.
25. Braun U, Plichta MM, Esslinger C, et al. Test-retest reliability of resting-state connectivity network characteristics using fMRI and graph theoretical measures. *NeuroImage* 2012; 59: 1404–1412.
26. Rubinov M and Sporns O. Complex network measures of brain connectivity: Uses and interpretations. *NeuroImage* 2010; 52: 1059–1069.
27. Ostergaard L, Weisskoff RM, Chesler DA, et al. High resolution measurement of cerebral blood flow using intravascular tracer bolus passages. Part I: mathematical approach and statistical analysis. *Magn Reson Med* 1996; 36: 715–725.
28. Heaton RK, Ryan L and Grant I. *Demographic influences and use of demographically corrected norms in neuropsychological assessment*. *Neuropsychological assessment of neuropsychiatric and neuromedical disorders*, 3rd ed. New York: Oxford University Press, 2009, pp.127–155.
29. Ferreira LK, Regina ACB, Kovacevic N, et al. Global functional connectivity is related to age and memory performance in healthy adults: a resting-state fMRI study. *J Neurol Sci* 2013; 333: e726.
30. Wang J, Zuo X and He Y. Graph-based network analysis of resting-state functional MRI. *Front Syst Neurosci* 2010; 4: 16.
31. van Wijk BC, Stam CJ and Daffertshofer A. Comparing brain networks of different size and connectivity density using graph theory. *PLOS One* 2010; 5: e13701.
32. Christen T, Jahanian H, Ni WW, et al. Noncontrast mapping of arterial delay and functional connectivity using resting-state functional mri: a study in moyamoya patients. *J Magn Reson Imaging* 2015; 41: 424–430.
33. Binnewijzend MAA, Schoonheim MM, Sanz-Arigita E, et al. Resting-state fMRI changes in alzheimer's disease and mild cognitive impairment. *Neurobiol Aging* 2012; 33: 2018–2028.
34. Rombouts SARB, Barkhof F, Goekoop R, et al. Altered resting state networks in mild cognitive impairment and mild alzheimer's disease: an fMRI study. *Hum Brain Mapp* 2005; 26: 231–239.
35. Latora V and Marchiori M. Efficient behavior of small-world networks. *Phys Rev Lett* 2001; 87: 198701.
36. Watts DJ and Strogatz SH. Collective dynamics of 'small-world' networks. *Nature* 1998; 393: 440–442.
37. Newman ME. Modularity and community structure in networks. *Proc Nati Acad Sci U S A* 2006; 103: 8577–8582.
38. de Haan W, Pijnenburg Y, Strijers R, et al. Functional neural network analysis in frontotemporal dementia and alzheimer's disease using eeg and graph theory. *BMC Neurosci* 2009; 10: 101.
39. Kim S-G and Ogawa S. Biophysical and physiological origins of blood oxygenation level-dependent fMRI signals. *J Cereb Blood Flow Metab* 2012; 32: 1188–1206.
40. Chang TY, Kuan WC, Huang KL, et al. Heterogeneous cerebral vasoreactivity dynamics in patients with carotid stenosis. *PLOS One* 2013; 8: e76072.